

Get Clarity On Generics

Cost-Effective CT & MRI Contrast Agents



FRESENIUS
KABI

WATCH VIDEO

AJNR

Distal Vessel Imaging via Intra-arterial Flat Panel Detector CTA during Mechanical Thrombectomy

T. Nozaki, M. Noda, T. Ishibashi, K. Otani, M. Kogiku, K. Abe, H. Kishi and A. Morita

This information is current as of August 10, 2025.

AJNR Am J Neuroradiol published online 24 December 2020

<http://www.ajnr.org/content/early/2020/12/24/ajnr.A6906>

Distal Vessel Imaging via Intra-arterial Flat Panel Detector CTA during Mechanical Thrombectomy

 T. Nozaki,  M. Noda,  T. Ishibashi,  K. Otani,  M. Kogiku,  K. Abe,  H. Kishi, and  A. Morita



ABSTRACT

BACKGROUND AND PURPOSE: Obtaining information on invisible vasculature distal to the occlusion site helps to deploy a stent retriever safely during mechanical thrombectomy for large-vessel occlusion. It is essential to reduce the amount of contrast used for detecting the vessels distal to the occlusion site because acute ischemic stroke patients tend to have chronic kidney disease and patients with severe chronic kidney disease are at an increased risk of contrast-associated acute kidney injury. We assessed whether vessels distal to the occlusion site during acute ischemic stroke with large-vessel occlusion could be visualized on angiographic images using flat panel detector CT acquired following intra-arterial diluted contrast injection, compared with MRA findings.

MATERIALS AND METHODS: Between May 2019 and January 2020, we enrolled 28 consecutive patients with large-vessel occlusions of the anterior circulation eligible for mechanical thrombectomy following MR imaging. The patients underwent CBV imaging using flat panel detector CT with an intra-arterial diluted contrast injection instead of intravenous injection. Flat panel detector CT angiographic images reconstructed from the same dataset were evaluated for image quality, collateral status of the MCA territory, and visualization of the vessels distal to the occlusion site. These findings were compared with MRA findings.

RESULTS: Twenty-two patients were retrospectively examined. Flat panel detector CT angiographic image quality in 20 patients (91%) was excellent or good. The distal portion of the occluded vessel segment was visualized in 14 patients (70%), while the proximal portion of the segment adjacent to the occluded vessel in 3 (15%) was visualized. No visualization was observed in only 1 patient (5%) with no collateral supply. Flat panel detector CT angiographic images were shown to evaluate vessels distal to the occlusion site more accurately than MRA.

CONCLUSIONS: In acute ischemic stroke with large-vessel occlusion, flat panel detector CT angiographic images could successfully visualize vessels distal to the occlusion site with a small amount of contrast material.

ABBREVIATIONS: AIS = acute ischemic stroke; cICA = cervical ICA; FPD = flat panel detector; ICA-T = ICA terminal; LVO = large-vessel occlusion; MT = mechanical thrombectomy

Mechanical thrombectomy (MT) using a stent retriever is an effective treatment strategy for acute ischemic stroke (AIS) with large-vessel occlusion (LVO).¹⁻⁴ Obtaining information on invisible vasculature distal to the occlusion site helps to select appropriate devices and guides them safely because MT, using a stent retriever, requires a microguidewire and microcatheter to

pass through the occlusion site and be guided to an invisible vessel distal to the occlusion site. Furthermore, a stent retriever must be deployed, usually in an invisible vessel. Approximately 20%–35% of patients with AIS have chronic kidney disease,⁵ and patients with severe chronic kidney disease are at an increased risk of contrast-associated acute kidney injury.^{6,7} Therefore, it is essential to reduce the amount of contrast used for diagnostic imaging. Pial collaterals can be assessed using CTA.⁸⁻¹⁰ Similarly, flat panel detector (FPD) CT angiography in the angiography suite¹¹ following intravenous contrast injection allows detecting vessels distal to the occlusion site. Furthermore, FPD CT has also been used to generate FPD CBV images with an intravenous contrast injection,¹² which are potentially useful for prediction of the final infarct volume in patients with AIS with LVO¹³⁻¹⁵ and of hemorrhagic infarction post-MT.¹⁶ The image reconstruction of FPD CBV datasets provides FPD CT

Received June 27, 2020; accepted after revision September 5.

From the Department of Neurosurgery (T.N., M.N., M.K., K.A., H.K.), Yokohama Shin-Midori General Hospital, Kanagawa, Japan; Department of Neurological Surgery (T.N., A.M.), Nippon Medical School Hospital, Tokyo, Japan; Department of Neurosurgery (T.I.), Jikei University School of Medicine, Tokyo, Japan; and Siemens Healthcare K.K. (K.O.), Tokyo, Japan.

Please address correspondence to Toshiki Nozaki, MD, Department of Neurological Surgery, Nippon Medical School Hospital, 1-1-5 Sendagi, Bunkyo-ku, Tokyo 113-8603, Japan; e-mail: tonod03sm069@gmail.com



Indicates article with supplemental online photos.

<http://dx.doi.org/10.3174/ajnr.A6906>

angiographic images that are comparable with CTA with regard to the visualization of LVO, collateral state, and clot extent.¹² Moreover, FPD CBV images can be obtained using an intra-arterial diluted contrast injection,^{16,17} which requires less contrast material. However, it remains unclear whether the vessels distal to the occlusion site in patients with stroke can be evaluated on the FPD CT angiographic images with intra-arterial diluted contrast injection.

Therefore, in our study, we assessed whether FPD CT angiographic images, generated during FPD CBV imaging with an intra-arterial diluted contrast injection, could visualize vessels distal to the occlusion site in patients with AIS compared with MRA findings.

MATERIALS AND METHODS

This study was approved by the ethics committee of Yokohama Shin-Midori General Hospital (permission No. 19001-2) and was performed using the opt-out method described on our hospital Web site.

Subjects and Methods

Between May 2019 and January 2020, we enrolled all patients with AIS with LVO of the anterior circulation (ICA and MCA) who were eligible for MT. An MR imaging-based protocol was used to select patients for reperfusion therapy (Online Fig 1). All patients, except those for whom MR imaging was contraindicated, were assessed using MR imaging and MRA to diagnose AIS and LVO. Nonenhanced CT was used to evaluate AIS and exclude hemorrhage or large demarcated infarction in patients contraindicated for MR imaging. Following assessment using MR imaging/MRA or a nonenhanced CT, all patients were treated with IV rtPA therapy in the angiography suite, when eligible. An 8F sheath was inserted into the femoral artery following groin puncture. Then, an 8F balloon guide catheter and a 6F diagnostic catheter coaxial system were used, and FPD CBV images were acquired. The extent of tissue damage was assessed on MR imaging before the procedure. We used the FPD CBV images to confirm the extent of damaged brain tissue and to assess risks of hyperperfusion and hemorrhagic infarction following the procedure, and we used the FPD CT angiography images as reference vessel images for performing MT.

FPD CBV and MRA Imaging Protocols

MRA imaging was performed with a 1.5T MR imaging scanner (EXCELRT Vantage; Canon Medical Systems) using a TOF-MRA sequence (TE = 6.8 ms, TR = 21 ms, flip angle = 18°, FOV = 200 × 200 mm, section thickness = 1 mm, pixel spacing = 1.3 × 0.8, resulting in an acquisition time = 4 minutes and 12 seconds).

We used a biplanar flat panel detector angiographic system (Artis zee biplane VD11C; Siemens) for all angiographic imaging. FPD CBV imaging was performed with 2 rotations of the flat panel detector system. Mask images (mask run) were first acquired and fill images (fill run) were acquired post-contrast injection. We applied the following protocol:^{16,18} acquisition time, 6 seconds; x-ray tube voltage, 70 kV; total angle, 200°; projections, 400; dose, 0.36 mGy/

frame; and x-ray delay, 9 seconds. We used contrast medium with an iodine concentration of 300 mg/mL. A solution of 30% diluted contrast medium was injected using a power injector at a rate of 6.0 mL/s through a 6F diagnostic catheter placed just above the aortic valve in the ascending aorta. The total contrast dose was 25.2 mL (total injection volume was 84 mL). Two types of images were generated simultaneously: angiographic images reconstructed from the fill run (FPD CT angiographic images), and color-coded FPD CBV images from the mask and fill runs (Fig 1A) using the application software of the workstation of the system (syngo DynaPBV Neuro; Siemens). The color-coded FPD CBV images provided an approximation of the CBV and a real-time overview on the extension of irreversibly damaged brain tissue. The additional FPD CT angiographic images depicted intracranial vessels post-contrast flow in the brain parenchyma reached a steady-state, and were used for detecting LVO and vessels distal to the occlusion site, evaluating the collateral status of the occluded MCA territory during MT.

Image Analysis

All images were anonymized before analysis and evaluated by 2 board-certified and experienced neurosurgeons (H.K. and M.N.) blinded to clinical information. Vessels proximal to the occlusion site were identified on FPD CT angiographic images and initial MRA and described as follows: cervical ICA (cICA); ICA terminal (ICA-T); MCA M1 segment (M1) proximal/distal; and MCA M2 segment (M2) proximal/distal. Previously published scales of angiographic assessment were used.

First, we evaluated the image quality of FPD CT angiographic images on a 4-point scale:¹⁹ 1) poor image quality, blurring of the vessel contours; 2) fair image quality, suboptimal arterial enhancement for confident diagnosis; 3) good image quality and arterial enhancement, adequate for confident diagnosis; and 4) excellent image quality and arterial enhancement.

We evaluated the visualization of vessels distal to the occlusion site on the basis of retrograde contrast opacification of vessels within the occluded territory on FPD CT angiographic images and MRA.²⁰ The visualization score, used to assess the degree of visualization of vessels distal to the occlusion site, consisted of 5 categories describing which part of the collateral vessels could be visualized: 1) distal portion of the occluded vessel segment, 2) proximal portion of the segment adjacent to the occluded vessel, 3) distal portion of the segment adjacent to the occluded vessel, 4) vessels 2 segments distal to the occluded vessel, and 5) little-or-no significant visualization of the territory of the occluded vessel. For example, in the case of M1 proximal occlusion, if M1 distal was visualized, a score of 1 was assigned. Similarly, if the M2 proximal, M2 distal, or MCA M3 segment was visualized, a score of 2, 3, or 4 was, respectively, assigned. Online Fig 2 shows the visualization score rating, for example, in the case of right ICA-T occlusion.

Finally, the collateral status of the occluded MCA territory was evaluated semiquantitatively on the same FPD CT angiographic images and scored on a 4-point scale:²¹ 0) absent collateral supply

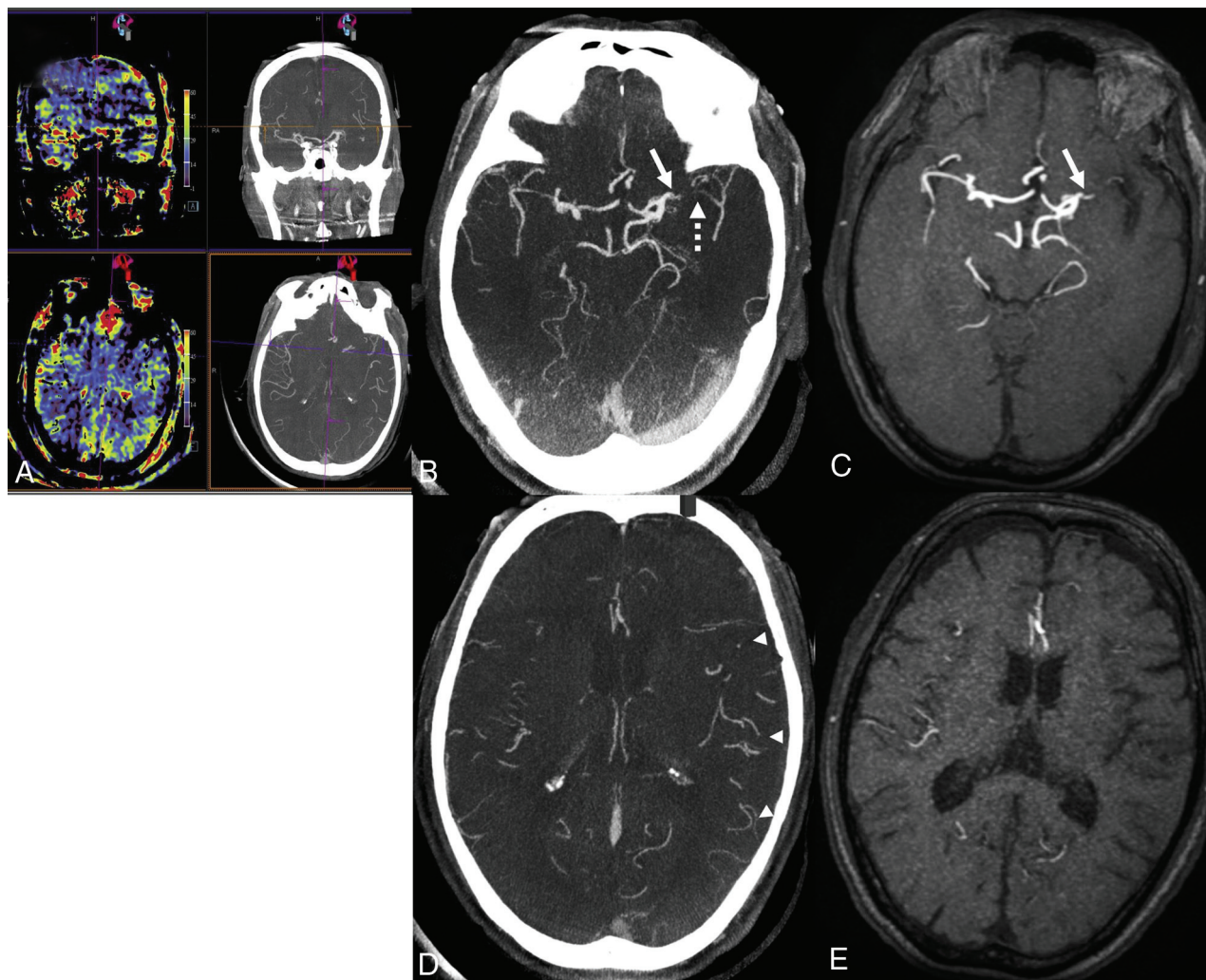


FIG 1. Representative case 1. A patient presented with a left M1 segment occlusion. A, FPD CBV imaging includes FPD CBV images and FPD CT angiographic images. B, The axial FPD CT angiographic images could visualize the occlusion site (M1 proximal, *white continuous arrow*) and its distal vessel (M1 distal, *white dashed arrow*) by the filling of collaterals. The visualization score is 1. C, MRA could visualize the occlusion site but not its distal vessel (visualization score = 5). D, *White arrowheads* in the FPD CT angiographic image show the filling of the MCA territory via leptomeningeal anastomosis. The collateral score is 3 for 100% collateral supply of the occluded MCA territory. E, The filling of the MCA territories is not confirmed on the MRA. MIP thickness is set to 10 mm for B and C and 5 mm for D and E.

to the occluded MCA territory, 1) collateral supply filling $\leq 50\%$ but $>0\%$ of the occluded MCA territory, 2) collateral supply filling $>50\%$ but $<100\%$ of the occluded MCA territory, and 3) 100% collateral supply of the occluded MCA territory.

MIP thickness of FPD CT angiographic images was changed from 1 to 99 mm according to the rater's intention when assessing the visualization score and fixed to 5 mm when assessing the collateral score.

Statistical Analysis

Interrater agreement was analyzed using the quadratic weighted κ statistic (≤ 0.4 , poor agreement; $0.4-0.75$, fair to good agreement; ≥ 0.75 , excellent agreement²²). The Spearman rank correlation coefficient, the Mann-Whitney U test, and the Kruskal-Wallis test followed by the Steel-Dwass post hoc test were used to assess associations of the visualization score with the collateral score, the occlusion site, TICI grade, and the 90-day mRS. The Mann-Whitney U test was used to assess the difference in the visualization

scores between FPD CT angiographic images and MRA. The level of statistical significance was set to $P < .05$. Data from the more experienced of the 2 raters have been used in the text, tables, and figures. Statistical software (Easy R [EZR]; Saitama Medical Center, Jichi Medical University) was used for all statistical analyses.

RESULTS

We performed MT for 28 consecutive patients with AIS with LVO of the anterior circulation. Six of them did not undergo FPD CBV imaging because 2 were treated in the other angiography suite where we could not perform FPD CBV imaging, and 4 were excluded owing to a protocol violation. Therefore, the remaining 22 patients underwent FPD CBV imaging and were retrospectively analyzed.

Patient Characteristics

Table 1 shows the baseline characteristics of the 22 patients who fulfilled the inclusion criteria. Twenty patients were

initially assessed by MR imaging and MRA. The remaining 2 patients with cardiac pacemaker implantation were initially assessed by nonenhanced CT. Of the 22 patients, 2 patients (9%) had a cerebral aneurysm: One had an aneurysm at the bifurcation of M1–M2 distal to the occlusion site (ICA-T), which was not depicted owing to its fair image quality caused by motion artifacts, while the other had an aneurysm at the bifurcation of M1–M2 proximal to the occlusion site (M2 proximal), which was visualized using FPD CT angiographic images.

Evaluation of FPD CT Angiographic Images

Table 2 shows the results of the FPD CT angiographic image evaluation of all patients. The proximal occluded sites identified on

FPD CT angiographic images and initial MRA were ICA-T ($n = 7$), M1 proximal ($n = 4$), M1 distal ($n = 2$), M2 proximal ($n = 6$), M2 distal ($n = 1$), cICA and M2 proximal (tandem occlusions) ($n = 2$). In 2 cases of tandem occlusions with cICA and M2 proximal, vessels distal to the occlusion site (M2 proximal) were observed on FPD CT angiographic images only, not on MRA. The FPD CT angiographic images of 20 patients (91%) had good or excellent image quality, and the FPD CT angiographic images of 2 patients (9%) had poor or fair image quality owing to motion artifacts.

The vessels distal to the occlusion site were visualized only in the 20 patients with good or excellent image quality as follows: the distal portion of the occluded vessel segment (visualization score = 1) in 14 patients (70%), the proximal portion of the segment adjacent to the occluded vessel (visualization score = 2) in 3 patients (15%), and the distal portion of the segment adjacent to the occluded vessel (visualization score = 3) in 2 patients (10%). Only 1 patient (5%) who had no collateral supply (collateral score = 0) had no significant visualization of the territory of the occluded vessel (visualization score = 5).

Evaluation of the Visualization Score Using MRA

We evaluated the MRA scans of 20 patients; 2 patients contraindicated for MR imaging were excluded. The visualization scores were 2 in 1 patient (5%), 3 in 2 patients (10%), 4 in 2 patients (10%), and 5 in 15 patients (75%).

Statistical Analyses for Visualization Score

FPD CT angiographic images were shown to evaluate the visualization score more accurately than MRA (median scores, FPD CT versus MRA = 1 and 5, $P < .001$) in 19 patients with good- or excellent-quality FPD CT angiographic images. Vessels distal to the

occlusion site were significantly more clearly visualized in patients with MCA M1 and M2 occlusion than in patients with ICA occlusion (median scores, M1 = 1, M2 = 1, ICA = 2; M1 versus ICA, $P = .01$; M2 versus ICA, $P = .007$). There was a significant correlation between the visualization scores and collateral scores ($r = -0.61$, $P = .004$) and between the visualization scores and the 90-day mRS after MT ($r = 0.49$, $P = .03$). In contrast, the TICI grade did not significantly correlate with the visualization scores ($P = .39$).

Interrater agreement analyzed by the quadratic weighted κ statistic was excellent for image quality, visualization score, and collateral scores (0.85, 0.90, and 0.80, respectively).

Representative Cases

Case 1: M1 Occlusion, Patient No. 8. A patient presented with a left M1

Table 1: Baseline characteristics^a

Characteristics	
Patient background	
Age (yr)	74.9 [SD, 13.1]
Atrial fibrillation	16 (72.7%)
Hypertension	13 (59.1%)
Diabetes mellitus	2 (9.1%)
Dyslipidemia	12 (54.5%)
Chronic kidney disease	11 (50%)
Clinical status and treatment	
NIHSS at arrival	13.9 [SD, 5.9]
Sedation (midazolam)	6 (27.3%)
IV rtPA therapy	8 (40.9%)
TICI Grade 2a	1 (4.5%)
Grade 2b	5 (22.7%)
Grade 3	16 (72.7%)
Puncture-to-recanalization time (min)	66.2 [SD, 25.2]
Total contrast dose (mL)	130.3 [SD, 39.4]
mRS pre-onset	0.6 [SD, 1.2]
90-day post-MT	2.7 [SD, 1.9]

^a Data are presented as mean [SD] or No. (%).

Table 2: Results of FPD CT angiographic image and MRA evaluation

Patient No.	Occlusion Site	Image Quality	Collateral Score	Visualization Score	
				FPD CT	MRA
1	ICA-T	Excellent	1	3	3
2	ICA-T	Excellent	3	2	5
3	ICA-T	Poor	—	—	—
4	ICA-T	Excellent	1	3	5
5	ICA-T	Excellent	1	2	—
6	ICA-T	Fair	—	—	5
7	ICA-T	Excellent	0	5	5
8	M1 proximal	Excellent	3	1	5
9	M1 proximal	Excellent	2	1	5
10	M1 proximal	Excellent	2	1	5
11	M1 proximal	Excellent	2	1	4
12	M1 distal	Excellent	3	1	5
13	M1 distal	Good	2	1	3
14	M2 proximal	Excellent	3	1	4
15	M2 proximal	Good	1	1	2
16	M2 proximal	Excellent	2	1	5
17	M2 proximal	Excellent	2	1	5
18	M2 proximal	Excellent	2	1	5
19	M2 proximal	Good	2	1	5
20	M2 distal	Excellent	3	1	5
21	cICA, M2 proximal	Good	3	1	5
22	cICA, M2 proximal	Good	1	2	5

Note: — indicates unevaluable.

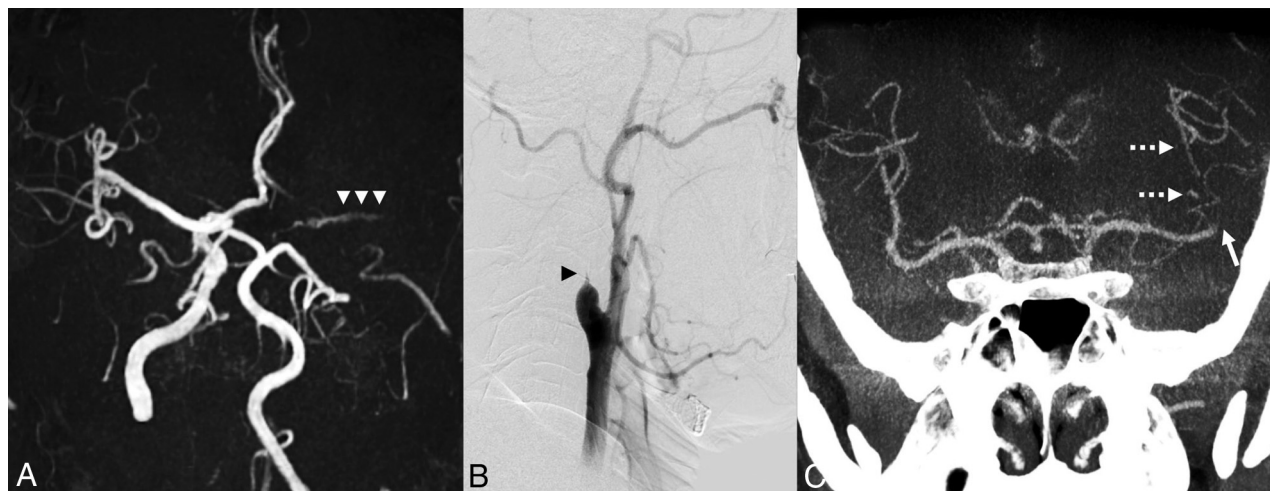


FIG 2. Representative case 2. A patient presented with tandem occlusions (cICA and M2 segment proximal occlusions). A, The left intracranial ICA is not visualized on MRA, suggesting left cICA occlusion. White arrowheads show slightly depicted M1 segment probably via the anterior communicating artery. Left M2 occlusion could not be identified on MRA. B, FPD CBV imaging before percutaneous transluminal angioplasty followed by conventional angiography at the left common carotid artery identifies left cICA occlusion (black arrowhead). C, The occlusion site (M2 proximal, white continuous arrow) and its distal vessel (M2 distal, white dashed arrows) on the coronal image by the fillings of collaterals. The visualization score is 1. MIP thickness is set to 20 mm.

proximal occlusion at 85 minutes with an NIHSS score of 29 (Fig 1). Concurrent with IV rtPA, MT using the stent retriever and reperfusion catheter was performed. TICI 3 recanalization was achieved 32 minutes post-groin puncture. FPD CT angiographic images could visualize the occlusion site (M1 proximal) and its distal vessel (M1 distal) by the filling of collaterals. We evaluated the visualization score as 1 and the collateral score as 3.

Case 2: cICA and M2 Occlusions, Patient No. 21. A patient presented with tandem occlusions with cICA and M2 proximal occlusion at 177 minutes, with an NIHSS score of 6 (Fig 2). MRA showed that left cICA occlusion was suspected; thus, we subsequently performed FPD CBV imaging in the angiography suite. FPD CT angiographic images revealed an M2 proximal occlusion. Concurrent with IV rtPA, percutaneous transluminal angioplasty using an angioplasty balloon for the cICA occlusion and MT using a stent retriever for the M2 occlusion were performed sequentially. The groin puncture to target recanalization time for M2 occlusion was 70 minutes, and TICI 3 recanalization was achieved. Contrast medium for FPD CBV imaging was administered from the ascending aorta just above the aortic valve before percutaneous transluminal angioplasty. FPD CT angiographic images could visualize the occlusion site (M2 proximal) and its distal vessel (M2 distal) by the filling of collaterals, though initial MRA did not show the occlusion site (M2 proximal). We evaluated the visualization score as 1. The images allowed planning for target recanalization (M2 occlusion) early during the procedure. Therefore, conventional angiography with contrast injection could be reduced, and some selective guidance of the catheter to specific vessels could be omitted.

DISCUSSION

In this study, we investigated whether vessels distal to the occlusion site in patients with AIS with LVO can be detected before MT on FPD CT angiographic images acquired post-intra-arterial diluted contrast injection. We found that the image quality of the FPD CT angiographic images was adequate for diagnosis, except in 2 cases affected by motion artifacts. These cases showed that movement and motion artifacts could not always be avoided, even in sedated patients. We could delineate the vessels distal to the occlusion site of the anterior circulation, including aneurysms in 2 patients, on all FPD CT angiographic images that had good or excellent image quality, except in 1 patient with no collateral supply (collateral score = 0). Interrater agreement for image quality, visualization score, and collateral score was excellent.

Vessels distal to the occlusion site tended to be more clearly visualized in patients with MCA occlusion than in patients with ICA-T occlusion but could be detected in all patients who had at least slight collateral flow (more than collateral score 1). Our result, therefore, suggests that even if there is only slight collateral supply in vessels distal to the occlusion site, they can be seen on FPD CT angiographic images using an intra-arterial contrast injection.

We used MR imaging as the first choice in treating patients with stroke because it allowed us to correctly differentiate between stroke and nonstroke conditions. However, MRA could not visualize collateral blood flow because it may have been too subtle to be detected. FPD CT angiographic images were also better at depicting vessels distal to the occlusion site than MRA.

The visualization score, using FPD CT angiographic images, was significantly correlated with the collateral score

and 90-day mRS post-MT. This finding suggested that FPD CT angiographic images may be useful for predicting clinical outcome of patients with AIS.

Patients with AIS eligible for MT have a higher prevalence of cerebral aneurysm (3.7%) than a healthy reference population.²³⁻²⁵ FPD CT angiographic imaging thus appeared useful for the planning of appropriate treatment strategies, considering anatomic details that need careful attention.

The results of our study suggested that FPD CT angiographic imaging using an intra-arterial injection may reduce the contrast dose used for visualization of vessels distal to the occlusion site compared with other modalities. This is important because the prevalence of chronic kidney disease in patients with AIS tends to be higher than in the general population,⁵ and the total contrast dose required for the MT procedure is difficult to predict in individual patients. In our hospital, whenever possible, the patients with AIS do not receive contrast medium for diagnostic imaging outside the angiography suite. The contrast dose required to obtain FPD CT angiographic images in our study was only 25.2 mL. This compares with 187–189 mL of contrast (converted to iodine concentrations of 300 mg/mL) used during a CT-based protocol (CTA or CTP) including MT^{6,7,26} and 80 mL of contrast used for FPD CT with intravenous injection.^{11,12} The effective radiation dose of FPD CBV imaging is less than that of CTA and CTP.^{27,28}

Our study has some limitations. First, it was a retrospective study with a small sample size, which has selection bias. Therefore, larger prospective studies are warranted to validate our results. Second, we could not compare our results with those from CTA/CTP or FPD CT with an intravenous contrast injection because we used an MR imaging-based protocol for selection of patients for reperfusion therapy.

CONCLUSIONS

FPD CT angiographic images acquired post-intra-arterial contrast injection could visualize vessels distal to the occlusion site for patients with AIS with LVO of the anterior circulation using a small amount of contrast material.

ACKNOWLEDGMENTS

The authors thank Masayuki Arakawa (Chief Radiologic Technologist, Yokohama Shin-Midori General Hospital) for the technical assistance. We also thank Editage (<https://www.editage.jp>) for English language editing.

Disclosures: Katharina Otani—RELATED: Other: Siemens Healthcare K.K., Comments: Employee.

REFERENCES

- Albers GW, Marks MP, Kemp S, et al. **Thrombectomy for stroke at 6 to 16 hours with election by perfusion imaging.** *N Engl J Med* 2018;378:708–18 [CrossRef Medline](#)
- Van Den Berg LA, Dijkgraaf MG, Berkhemer OA, et al; MR CLEAN Investigators. **Two-year outcome after endovascular treatment for acute ischemic stroke.** *N Engl J Med* 2017;376:1341–49 [CrossRef Medline](#)
- Berkhemer OA, Fransen PS, Beumer D, et al; MR CLEAN Investigators. **A randomized trial of intraarterial treatment for acute ischemic stroke.** *N Engl J Med* 2015;372:11–20 [CrossRef Medline](#)
- Nogueira RG, Jadhav AP, Haussen DC, et al. **Thrombectomy 6 to 24 hours after stroke with a mismatch between deficit and infarct.** *N Engl J Med* 2018;378:11–21 [CrossRef Medline](#)
- Toyoda K, Ninomiya T. **Stroke and cerebrovascular diseases in patients with chronic kidney disease.** *Lancet Neurol* 2014;13:823–33 [CrossRef Medline](#)
- Loh Y, McArthur DL, Vespa P, et al. **The risk of acute radiocontrast-mediated kidney injury following endovascular therapy for acute ischemic stroke is low.** *AJNR Am J Neuroradiol* 2010;31:1584–87 [CrossRef Medline](#)
- Diprose WK, Sutherland LJ, Wang MTM, et al. **Contrast-associated acute kidney injury in endovascular thrombectomy patients with and without baseline renal impairment.** *Stroke* 2019;50:3527–31 [CrossRef Medline](#)
- Smit EJ, Vonken EJ, Van Seeters T, et al. **Timing-invariant imaging of collateral vessels in acute ischemic stroke.** *Stroke* 2013;44:2194–99 [CrossRef Medline](#)
- Maas MB, Lev MH, Ay H, et al. **Collateral vessels on CT angiography predict outcome in acute ischemic stroke.** *Stroke* 2009;40:3001–05 [CrossRef Medline](#)
- Puetz V, Dzialowski I, Hill MD, et al. **Intracranial thrombus extent predicts clinical outcome, final infarct size and hemorrhagic transformation in ischemic stroke: the clot burden score.** *Int J Stroke* 2008;3:230–06 [CrossRef Medline](#)
- Blanc R, Pistocchi S, Babic D, et al. **Intravenous flat-detector CT angiography in acute ischemic stroke management.** *Neuroradiology* 2012;54:383–91 [CrossRef Medline](#)
- Hoelter P, Goelitz P, Lang S, et al. **Visualization of large vessel occlusion, clot extent, and collateral supply using volume perfusion flat detector computed tomography in acute stroke patients.** *Acta Radiol* 2019;60:1504–11 [CrossRef Medline](#)
- Ava L, Berkefeld J, Lauer A, et al. **Predictive value of pooled cerebral blood volume mapping for final infarct volume in patients with major artery occlusions. a retrospective analysis.** *Clin Neuroradiol* 2017;27:435–42 [CrossRef Medline](#)
- Fiorella D, Turk A, Chaudry I, et al. **A prospective, multicenter pilot study investigating the utility of flat detector derived parenchymal blood volume maps to estimate cerebral blood volume in stroke patients.** *J Neurointerv Surg* 2014;6:451–56 [CrossRef Medline](#)
- Wagner M, Kyriakou Y, du Mesnil de Rochemont R, et al. **Does preinterventional flat-panel computer tomography pooled blood volume mapping predict final infarct volume after mechanical thrombectomy in acute cerebral artery occlusion?** *Cardiovasc Intervent Radiol* 2013;36:1132–38 [CrossRef Medline](#)
- Moriya M, Itokawa H, Fujimoto M, et al. **Evaluation of patients with acute ischemic stroke using angiographic C-arm cerebral blood volume (C-arm CBV) measurements.** *Journal of Neuroendovascular Therapy* 2018;12:57–62 [CrossRef](#)
- Kuriyama T, Sakai N, Beppu M, et al. **Optimal dilution of contrast medium for quantitating parenchymal blood volume using a flat-panel detector.** *J Int Med Res* 2018;46:464–74 [CrossRef Medline](#)
- Ikemura A, Yuki I, Otani K, et al. **Evaluation of balloon test occlusion before therapeutic carotid artery occlusion: flat detector computed tomography cerebral blood volume imaging versus single-photon emission computed tomography.** *World Neurosurg* 2020; 133:e522–28 [CrossRef Medline](#)
- Hinkmann FM, Voit HL, Anders K, et al. **Ultra-fast carotid CT-angiography: low versus standard volume contrast material protocol for a 128-slice CT-system.** *Invest Radiol* 2009;44:257–64 [CrossRef Medline](#)
- Christoforidis GA, Mohammad Y, Kehagias D, et al. **Angiographic assessment of pial collaterals as a prognostic indicator following intra-arterial thrombolysis for acute ischemic stroke.** *AJNR Am J Neuroradiol* 2005;26:1789–97 [Medline](#)
- Tan IY, Demchuk AM, Hopyan J, et al. **CT angiography clot burden score and collateral score: correlation with clinical and radiologic**

- outcomes in acute middle cerebral artery infarct. *AJNR Am J Neuroradiol* 2009;30:525–31 [CrossRef Medline](#)
22. McCluggage WG, Bharucha H, Caughley LM, et al. Interobserver variation in the reporting of cervical colposcopic biopsy specimens: comparison of grading systems. *J Clin Pathol* 1996;49:833–35 [CrossRef Medline](#)
 23. Zhou T, Li T, Zhu L, et al. Endovascular thrombectomy for large-vessel occlusion strokes with preexisting intracranial aneurysms. *Cardiovasc Intervent Radiol* 2018;41:1399–403 [CrossRef Medline](#)
 24. Zibold F, Kleine JF, Zimmer C, et al. Aneurysms in the target vessels of stroke patients subjected to mechanical thrombectomy: prevalence and impact on treatment. *J Neurointerv Surg* 2016;8:1016–20 [CrossRef Medline](#)
 25. Vlak MH, Algra A, Brandenburg R, et al. Prevalence of unruptured intracranial aneurysms, with emphasis on sex, age, comorbidity, country, and time period: a systematic review and meta-analysis. *Lancet Neurol* 2011;10:626–36 [CrossRef Medline](#)
 26. Jia ZY, Wang SX, Zhao LB, et al. Risk of acute kidney injury with consecutive, multidose use of iodinated contrast in patients with acute ischemic stroke. *AJNR Am J Neuroradiol* 2019;40:652–54 [CrossRef Medline](#)
 27. Struffert T, Deuerling-Zheng Y, Kloska S, et al. Flat detector CT in the evaluation of brain parenchyma, intracranial vasculature, and cerebral blood volume: a pilot study in patients with acute symptoms of cerebral ischemia. *AJNR Am J Neuroradiol* 2010;31:1462–69 [CrossRef Medline](#)
 28. Struffert T, Deuerling-Zheng Y, Kloska S, et al. Dynamic angiography and perfusion imaging using flat detector CT in the angiography suite: a pilot study in patients with acute middle cerebral artery occlusions. *AJNR Am J Neuroradiol* 2015;36:1964–67 [CrossRef Medline](#)